



Since January 2020 Elsevier has created a COVID-19 resource centre with free information in English and Mandarin on the novel coronavirus COVID-19. The COVID-19 resource centre is hosted on Elsevier Connect, the company's public news and information website.

Elsevier hereby grants permission to make all its COVID-19-related research that is available on the COVID-19 resource centre - including this research content - immediately available in PubMed Central and other publicly funded repositories, such as the WHO COVID database with rights for unrestricted research re-use and analyses in any form or by any means with acknowledgement of the original source. These permissions are granted for free by Elsevier for as long as the COVID-19 resource centre remains active.



## Gamma-oryzanol as a potential modulator of oxidative stress and inflammation via PPAR- $\gamma$ in adipose tissue: a hypothetical therapeutic for cytokine storm in COVID-19?

Fabiane Valentini Francisqueti-Ferron<sup>a,\*</sup>, Jéssica Leite Garcia<sup>a</sup>, Artur Junio Togneri Ferron<sup>a</sup>, Erika Tiemi Nakandakare-Maia<sup>a</sup>, Cristina Schmitt Gregolin<sup>a</sup>, Janaina Paixão das Chagas Silva<sup>b</sup>, Klinsmann Carolo dos Santos<sup>a</sup>, Ângelo Thompson Colombo Lo<sup>a</sup>, Juliana Silva Siqueira<sup>b</sup>, Letícia de Mattei<sup>a</sup>, Bruno Henrique de Paula<sup>b</sup>, Felipe Sarzi<sup>c</sup>, Carol Cristina Vágula de Almeida Silva<sup>a</sup>, Fernando Moreto<sup>a</sup>, Mariane Róvero Costa<sup>a</sup>, Ana Lucia A. Ferreira<sup>a</sup>, Igor Otávio Minatel<sup>b</sup>, Camila Renata Corrêa<sup>a</sup>

<sup>a</sup> São Paulo State University (Unesp), Medical School, Botucatu, São Paulo, Brazil

<sup>b</sup> São Paulo State University (Unesp), Institute of Bioscience, Botucatu, São Paulo, Brazil

<sup>c</sup> Botucatu Integrated College (UNIFAC), Botucatu, São Paulo, Brazil

### ARTICLE INFO

**Keywords:**  
Obesity  
COVID-19  
Gamma-oryzanol  
PPAR- $\gamma$

### ABSTRACT

The literature has reported a higher prevalence of negative clinical outcomes due to Coronavirus disease 19 (COVID-19) in obese individuals. This can be explained by the cytokine storm, result from the cytokine production from both obesity and viral infection. Gamma-oryzanol ( $\gamma$ Oz) is a compound with anti-inflammatory and antioxidant activities. However, little is known about the  $\gamma$ Oz action as a possible agonist of peroxisome proliferator-activated receptor gamma (PPAR- $\gamma$ ). The aim of this study was to test the hypothesis that  $\gamma$ Oz attenuates the cytokine storm by stimulating PPAR- $\gamma$  in the adipose tissue. **Methods:** Male Wistar rats were randomly divided into three experimental groups and fed ad libitum for 30 weeks with control diet (C, n = 6), high sugar-fat diet (HSF, n = 6) or high sugar-fat diet +  $\gamma$ Oz (HSF +  $\gamma$ Oz, n = 6). HSF groups also received water + sucrose (25%). The  $\gamma$ Oz dose was 0.5% in the chow. Evaluation in animals included caloric intake, body weight, adiposity index, plasma triglycerides, and HOMA-IR. In adipose tissue was evaluated: PPAR- $\gamma$  gene and protein expression, inflammatory and oxidative stress parameters, and histological analysis. **Results:** Adipose tissue dysfunction was observed in HSF group, which presented remarkable PPAR- $\gamma$  underexpression and increased levels of cytokines, other inflammatory markers and oxidative stress. The  $\gamma$ Oz treatment prevented adipose tissue dysfunction and promoted PPAR- $\gamma$  overexpression. **Conclusion:** Natural compounds as  $\gamma$ Oz can be considered a coadjutant therapy to prevent the cytokine storm in COVID-19 patients with obesity conditions.

### 1. Introduction

Obesity comes from excessive body fat accumulation that progresses to severe health impairment (World Health Organization, 2017). Currently, obesity is considered a pandemic condition and a public health problem associated with increased risk for development of several complications and comorbidities as type 2 diabetes mellitus (DM2), hypertension, and dyslipidemia. In addition, these comorbidities

are associated to improved risk of kidney and cardiovascular diseases development (Francisqueti et al., 2015). All these functional or metabolic disorders has been established as risk factors for Coronavirus disease 2019 (COVID-19) and predictors of severity (Costa et al., 2020; Ayres, 2020). It has been known that obesity is implicated in systemic immunomodulatory effects that impair human metabolism and contributes to respiratory viral infection (Almond et al., 2013). Recent publications discuss the high prevalence of negative clinical outcomes

\* Corresponding author. Botucatu Medical School- UNESP, Av. Prof. Mário Rubens Guimarães Montenegro, s/n Bairro: Distrito de Rubião Junior 18.618-687, Botucatu, SP, Brazil.

E-mail addresses: [fabiane\\_vf@yahoo.com.br](mailto:fabiane_vf@yahoo.com.br), [fabiane.v.francisqueti@unesp.br](mailto:fabiane.v.francisqueti@unesp.br) (F.V. Francisqueti-Ferron).

<https://doi.org/10.1016/j.mce.2020.111095>

Received 7 August 2020; Received in revised form 23 November 2020; Accepted 24 November 2020

Available online 28 November 2020

0303-7207/© 2020 Elsevier B.V. All rights reserved.

due COVID-19 infection in obese individuals (Finer et al., 2020; Stefan et al., 2020; Chiappetta et al., 2020; Abbas et al., 2020). This prevalence can be explained by preexisting conditions that impair immune response or amplified pro-inflammatory responses triggered for obesity (Chiappetta et al., 2020). It is well established that obesity promotes a low-grade chronic systemic inflammation. However, when COVID-19 is associated to this condition, patients might develop a hyperinflammatory condition and the cytokine storm syndrome, which can lead to organs dysfunctions and failure, and even, death (Zabetakis et al., 2020; de Lucena et al., 2020).

The adipose tissue is a dynamic organ responsible not only by the fat storage, but it also exerts an endocrine role, secreting several adipokines that control the organism homeostasis (Birsoy et al., 2013; Manna and Jain, 2015). The adipokines include leptin, adiponectin, and inflammatory cytokines, in a complex network that physiologically regulates appetite, energy expenditure, peripheral insulin sensitivity, redox state, and lipid absorption in non-fat tissues (Francisqueti et al., 2015). However, in organisms under positive energetic balance, there is an adipose tissue hypertrophy, which is associated with disturbances in lipid metabolism and alterations in adipokines secretion, installing a pro-inflammatory state and oxidative stress. This adipose tissue dysfunction accelerates the development and progression of obesity-related insulin resistance and chronic diseases (Goossens and Blaak, 2015).

Efficient therapies or vaccines able to interrupt the severe acute respiratory syndrome coronavirus 2 (SARS-CoV-2) infection are still unavailable. In this meantime, the search for alternative therapies to modulate positively the immune response and the COVID-19 progression is urgent (Soy et al., 2020; Ciavarella et al., 2020). Several mechanisms have been studied around the world to find a strategy to control the virus insidious inflammatory effects. One of the most promisor mechanisms involves the peroxisome proliferator-activated receptor gamma (PPAR- $\gamma$ ) blockage. This nuclear receptor is highly expressed in adipose tissue and regulates the expression of several genes involved in adipocyte differentiation, lipid and carbohydrate metabolism, oxidative stress and inflammation (Fuentes et al., 2013). Considering this, a scientific study written by Ciavarella et al. (2020), reports that PPAR- $\gamma$  agonist substances may be candidates for cytokines storm modulation in COVID-19 disease (Ciavarella et al., 2020).

Natural compounds as  $\gamma$ Oz, the main bioactive from rice bran and germ, is a compound with anti-inflammatory and antioxidant activities (Minatel et al., 2016). Studies have shown that the  $\gamma$ Oz has a positive action in the treatment of some obesity-related comorbidities and attenuation of proinflammatory cytokines (Wang et al., 2015; Francisqueti et al., 2017a, 2018; Son et al., 2011). However, little is known about the  $\gamma$ Oz action as a possible agonist of PPAR- $\gamma$ . Thus, since this nuclear factor is synthesized by adipose tissue, the aim of this study was to test the hypothesis that  $\gamma$ Oz attenuates the cytokine storm by modulating the PPAR- $\gamma$  expression in the adipose tissue.

## 2. Methods

### 2.1. Experimental protocol

All the experiments and procedures were approved by the Animal Ethics Committee of Botucatu Medical School (process n° 1150/2015) and were performed in accordance with the National Institute of Health's Guide for the Care and Use of Laboratory Animals. Male Wistar rats ( $\pm 187$  g) were kept in an environmental controlled room ( $22 \text{ }^\circ\text{C} \pm 3 \text{ }^\circ\text{C}$ ; 12 h light-dark cycle and relative humidity of  $60 \pm 5\%$ ) and randomly divided into 3 experimental groups to receive: control diet (Control,  $n = 6$ ), high sugar-fat diet (HSF,  $n = 6$ ), or high sugar-fat diet +  $\gamma$ Oz (HSF +  $\gamma$ Oz,  $n = 6$ ) during 30 weeks. HSF groups also received water + sucrose (25%). The diets and water were ad libitum. The diets composition were based in our previous study (Francisqueti et al., 2017a).

### 2.2. Gamma-oryzanol

The compound was purchased from Tokyo Chemical Industry Co., Ltd. (Toshima, Kita-ku, Tokyo) (lot.5ZYZLPJ). Due to its nonpolar characteristics,  $\gamma$ Oz was added to diets to reach 0.5% of final concentration (w/w). This dose was based on the work of Son et al. (2011) and on the daily rice consumption of an adult individual in Brazil, according to data from the Family Budget Survey (POF) 2008–2009 (Instituto, 2011).

### 2.3. Nutritional parameters

The nutritional parameters included the following parameters: chow fed, water intake, caloric intake, final body weight, and adiposity index. Caloric intake was determined by multiplying the energy value of each diet (g  $\times$  Kcal) by the daily food consumption. For the HSF group, caloric intake also considered the calories from water ( $0.25 \times 4 \times \text{mL}$  consumed). Body weight was measured weekly. After euthanasia, the fat deposits (visceral (VAT), epididymal (EAT) and retroperitoneal (RAT)) were used to calculate the adiposity index (AI) by the following formula:  $[(\text{VAT} + \text{EAT} + \text{RAT})/\text{FBW}] \times 100$  (Francisqueti et al., 2018).

### 2.4. Metabolic and hormonal analysis

After 8-h fasting, blood was collected and the plasma was used to measure insulin and biochemical parameters. Glucose concentration was determined by using a glucometer (Accu-Chek Performa; Roche Diagnostics Brazil Limited); triglycerides was measured with an automatic enzymatic analyzer system (Chemistry Analyzer BS-200, Mindray Medical International Limited, Shenzhen, China). The insulin level was measured using the enzyme-linked immunosorbent assay (ELISA) method using commercial kits (EMD Millipore Corporation, Billerica, MA, USA). The homeostatic model of insulin resistance (HOMA-IR) was used as an insulin resistance index, calculated according to the formula:  $\text{HOMA-IR} = (\text{fasting glucose (mmol/L)} \times \text{fasting insulin } (\mu\text{U/mL}))/22.5$  (Francisqueti et al., 2018).

### 2.5. Systolic blood pressure

Systolic blood pressure (SBP) evaluation was assessed in conscious rats by the noninvasive tail-cuff method with a Narco Bio-Systems® electrophygmomanometer (International Biomedical, Austin, TX, USA). The animals were kept in a wooden box ( $50 \times 40$  cm) between 38 and  $40 \text{ }^\circ\text{C}$  for 4–5 min to stimulate arterial vasodilation (Santos et al., 2014). After this procedure, a cuff with a pneumatic pulse sensor was attached to the tail of each animal. The cuff was inflated to 200 mmHg pressure and subsequently deflated. The blood pressure values were recorded on a Gould RS 3200 polygraph (Gould Instrumental Valley View, Ohio, USA). The average of three pressure readings was recorded for each animal.

### 2.6. Structural and functional cardiac function by echocardiogram

Doppler echocardiographic evaluation was performed by a single examiner at the 30th week. Animals were anesthetized with ketamine (50 mg/kg, i. p.) and xylazine hydrochloride (1 mg/kg, i. p.). After trichotomy of the anterior chest region, the animals were placed in slight left lateral decubitus for the exam. The equipment used was model Vivid S6 (General Electric Medical Systems, Tirat Carmel, Israel) with a multifrequency ultrasonic transducer 5.0–11.5 MHz. To implement structural measurements of the heart, the images were obtained in one-dimensional mode (M-mode) guided by the images in two-dimensional mode with the transducer in the parasternal position, minor axis. Left ventricular (LV) evaluation was performed by positioning the cursor M-mode just below the mitral valve plane at the level of the papillary muscles. The images of the aorta and left atrium were obtained by

**Table 1**  
Nutritional, hormonal and cardiometabolic parameters.

	Control	HSF	HSF + $\gamma$ Oz
Chow fed (g/day)	24.41 $\pm$ 2.80 <sup>a</sup>	12.10 $\pm$ 2.24 <sup>b</sup>	10.45 $\pm$ 1.26 <sup>b</sup>
Water intake (ml/day)	34.22 $\pm$ 5.00 <sup>a</sup>	43.51 $\pm$ 2.41 <sup>b</sup>	44.39 $\pm$ 7.26 <sup>b</sup>
Caloric intake (kcal/day)	87.7 $\pm$ 10.0	94.8 $\pm$ 8.7	91.6 $\pm$ 8.2
Final body weight (g)	492 $\pm$ 58 <sup>a</sup>	591 $\pm$ 63 <sup>b</sup>	496 $\pm$ 58 <sup>a</sup>
Adiposity index (%)	4.53 $\pm$ 0.36 <sup>a</sup>	9.10 $\pm$ 1.95 <sup>b</sup>	6.33 $\pm$ 1.78 <sup>a</sup>
Fasting glucose (mg/dL)	74.8 $\pm$ 20.3 <sup>a</sup>	123 $\pm$ 7 <sup>b</sup>	93.7 $\pm$ 8.8 <sup>a</sup>
Insulin (ng/mL)	0.83 (0.77–0.83) <sup>a</sup>	3.80 (3.80–4.05) <sup>b</sup>	2.40 (2.10–2.80) <sup>b</sup>
HOMA-IR	6.02 $\pm$ 1.74 <sup>a</sup>	44.1 $\pm$ 7.7 <sup>b</sup>	18.3 $\pm$ 2.1 <sup>c</sup>
Triglycerides (mg/dL)	58.3 $\pm$ 16.1 <sup>a</sup>	117 $\pm$ 3 <sup>b</sup>	80.3 $\pm$ 12.5 <sup>c</sup>
Leptin (ng/mL)	0.45 $\pm$ 0.31 <sup>a</sup>	9.66 $\pm$ 1.09 <sup>b</sup>	2.60 $\pm$ 0.63 <sup>c</sup>
Adiponectin (ng/mL)	17918 $\pm$ 2548 <sup>a</sup>	31950 $\pm$ 1432 <sup>b</sup>	32443 $\pm$ 5174 <sup>b</sup>

positioning the M-mode course to plan the level of the aortic valve. The following cardiac structures were used to analyze cardiac morphology: left ventricular mass and relative wall thickness (RWT). The LV systolic function was assessed by the ejection fraction.

## 2.7. Adipose tissue evaluation

### 2.7.1. Preparation of the epididymal adipose tissue for analysis

Epididymal adipose tissue was selected for analysis due its similar inflammatory patterns to visceral fat (Francisqueti et al., 2017b). Four hundred milligrams of tissue were homogenized in 2.0 mL of Phosphate-Buffered saline (PBS) pH 7.4 cold solution ULTRA-TURRAX T25 basic IKA Werke Staufen/Germany, and centrifuged at 800 g at

4 °C for 10 min. The supernatant was used for inflammatory markers, MDA and protein carbonylation analysis, as follow:

### 2.7.2. Inflammatory markers

Tumoral necrosis factor-alpha (TNF- $\alpha$ ), interleukin-6 (IL-6) and monocyte chemoattractant protein- 1 (MCP-1) levels were measured using the enzyme-linked immunosorbent assay (ELISA) method using commercial kits from R&D System, Minneapolis, MN, USA (TNF- $\alpha$  DY510; IL-6 DY506; MCP-1 MJE00). The results were corrected by protein amounts.

## 2.8. Oxidative stress markers

### 2.8.1. Malondialdehyde levels (MDA)

MDA level was used to evaluate the lipid peroxidation. Briefly, 250  $\mu$ L of epididymal adipose tissue supernatant was used plus 750  $\mu$ L of 10% trichloroacetic acid for precipitation of proteins. Samples were centrifuged (3000 rpm; for 5 min; Eppendorf Centrifuge 5804-R, Hamburg, Germany) and the supernatant removed. Thiobarbituric acid (TBA) was added 0.67% in ratio (1:1) and the samples heated for 15 min at 100 °C. MDA reacts with TBA in the ratio 1:2 MDA-TBA, absorbed at 535 nm. After cooling, the reading at 535 nm was performed on Spectra Max 190 microplate reader (Molecular Devices, Sunnyvale, CA, USA). The MDA concentration was obtained by the molar extinction coefficient ( $1.56 \times 10^5 \text{ M}^{-1} \text{ cm}^{-1}$ ) and the absorbance of the samples and the final result expressed in nmol/g protein (Samarghandian et al., 2016).

### 2.8.2. Protein carbonylation

Carbonylated proteins were measured by an unspecific method that

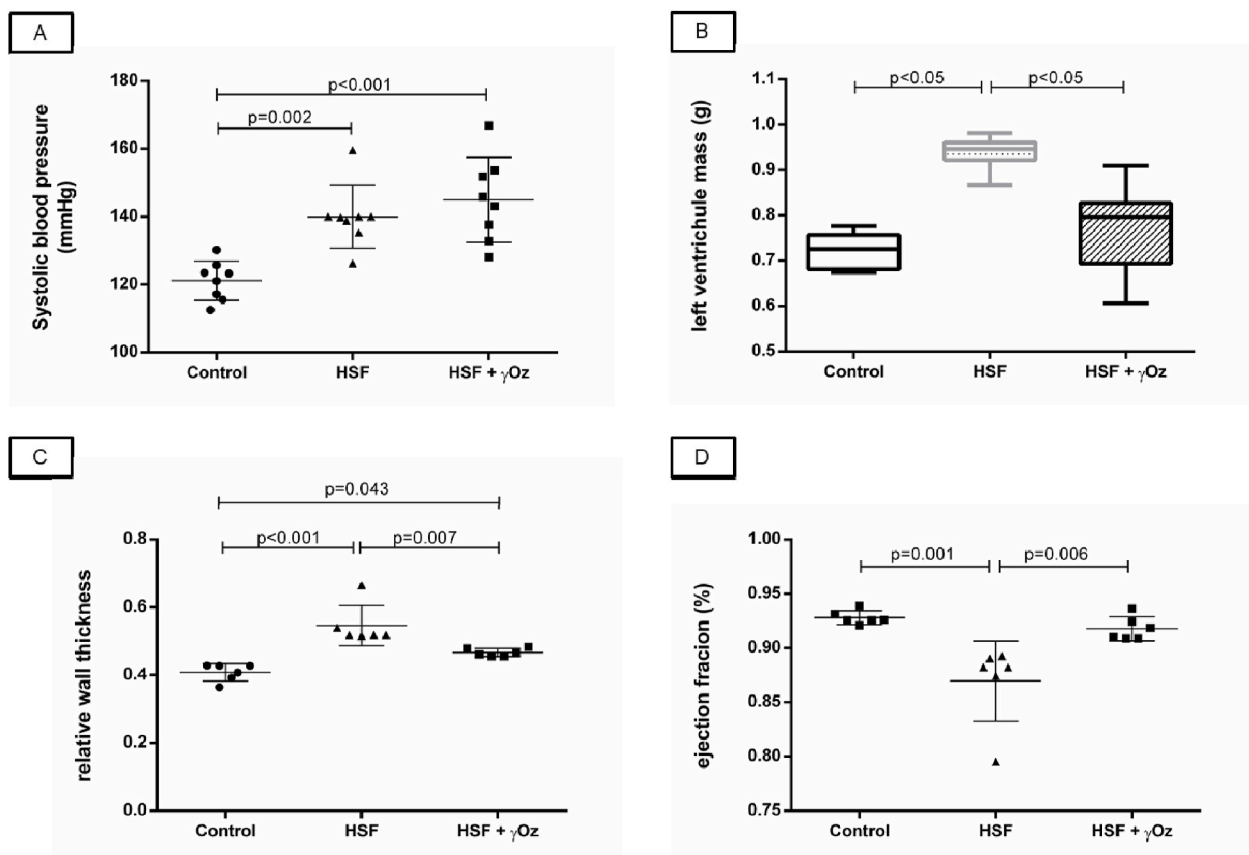


**Fig. 1.** Systolic blood pressure and echocardiogram parameters. A- systolic blood pressure (mmHg); B- left ventricular mass (g); C- Relative wall thickness; D- ejection fraction (%). Data are presented as means  $\pm$  standard deviation. Comparison by One-way ANOVA with Tukey post-hoc. HSF—high sugar-fat diet.  $\gamma$ Oz—Gamma-oryzanol.

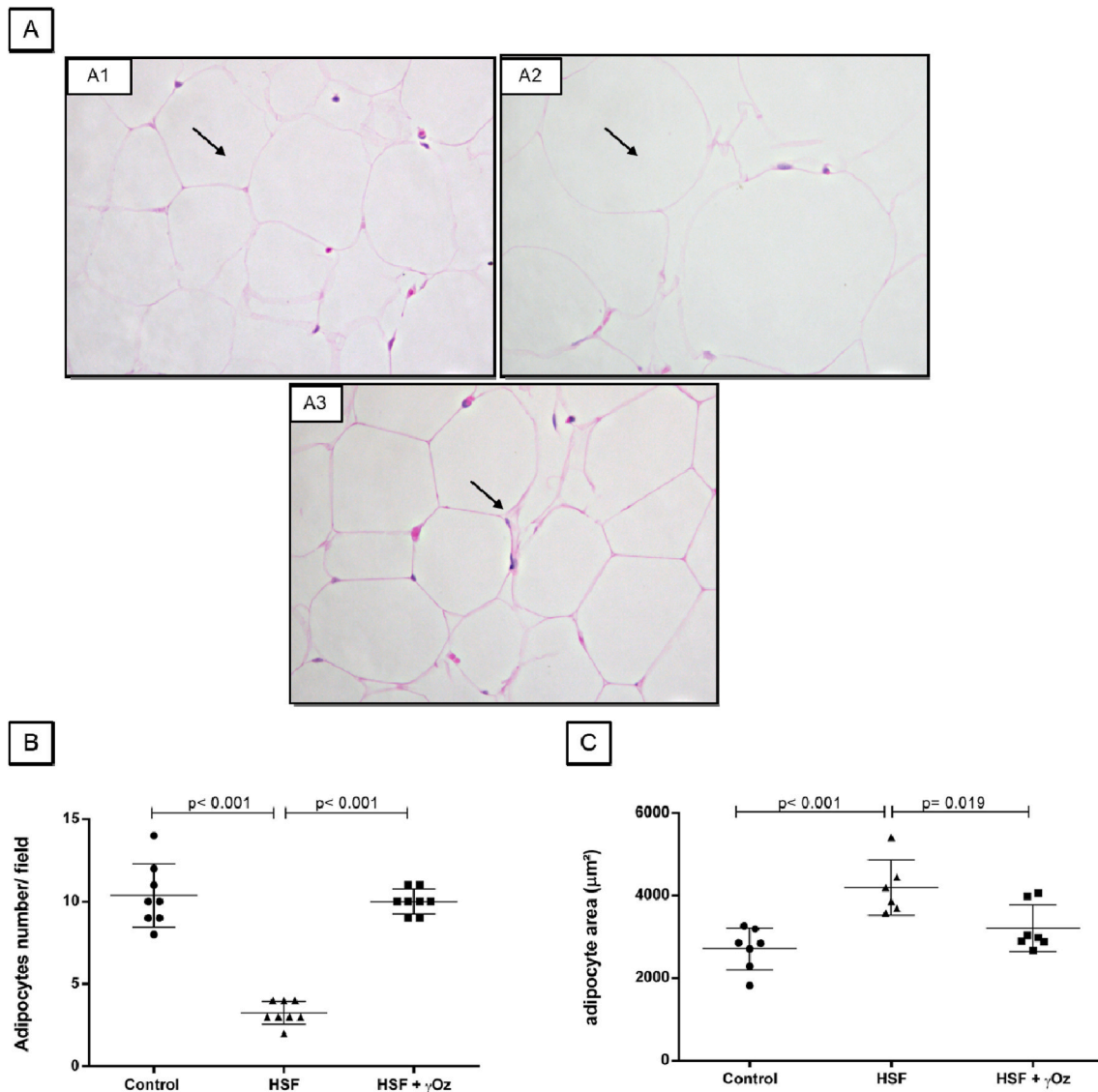


**Fig. 2.** Histological analysis of adipose tissue. A- Adipocytes- histological section of adipose tissue colored by hematoxylin-eosin. A1- Control; A2- HSF; A3- HSF +  $\gamma$ Oz; B- adipocytes number by field. C- Adipocyte area ( $\mu\text{m}^2$ ). Data are expressed in mean  $\pm$  standard deviation. Comparison by One-way ANOVA with Tukey post-hoc. HSF—high sugar- fat diet.  $\gamma$ Oz—Gamma-oryzanol. Analysis were made under 40x magnification.

uses DNPH (2,4-dinitrophenylhydrazine derivatizing agent) and photometric detection of any modified protein by carbonylation (Mesquita et al., 2014). Carbonylated proteins levels are expressed in nmol of DNPH/mg of protein.

## 2.9. Adipose tissue hypertrophy and hyperplasia

### 2.9.1. Histological analysis

Adipose tissue was fixed in 4% formaldehyde and embedded in paraffin. Two consecutive sections from each sample were cut (4  $\mu\text{m}$ ) and stained with hematoxylin/eosin. The entire slide was scanned using LEICA DM LS microscope coupled to a video camera that captures the digital image and sends it to a computer, compatible IBM PC, equipped with image analysis program Image Pro-plus (Media Cybernetics, Silver spring, Maryland USA) (Francisqueti et al., 2017b). The mean area of adipocytes was calculated using a method previously described by Osman in 2013 (Osman et al., 2013). Using the same slide, it was also counted the number of cells per field. The analyses were performed under 40X magnification.

## 2.10. PPAR- $\gamma$ evaluation

### 2.10.1. Real-time PCR

Total RNA was extracted from epididymal adipose tissue using the reagent TRIzol (Invitrogen). The SuperScript II First-Strand Synthesis System for RT-PCR (Invitrogen) kit was used for the synthesis of 20  $\mu\text{l}$  of complementary DNA from 1000 ng of total RNA. The mRNA levels of PPAR- $\gamma$  (Rn00440945\_m1, Applied Biosystems) was determined by real-time PCR. Quantitative measurements were made with a commercial kit (TaqMan qPCR; Applied Biosystems) in a detection system (StepOne Plus; Applied Biosystems). Cycling conditions were as follows: enzyme activation at 50  $^{\circ}\text{C}$  for 2 min, denaturation at 95  $^{\circ}\text{C}$  for 10 min, complementary DNA products were amplified for forty cycles of denaturation at 95  $^{\circ}\text{C}$  for 15 s and annealing/extension at 60  $^{\circ}\text{C}$  for 1 min. Gene expression was quantified in relation to the values of the C group after normalization by an internal control (cyclophilin: assay Rn 00690933\_m1; Applied Biosystems) by the method  $2^{-\Delta\Delta\text{C T}}$ , as described previously (Livak and Schmittgen, 2001).

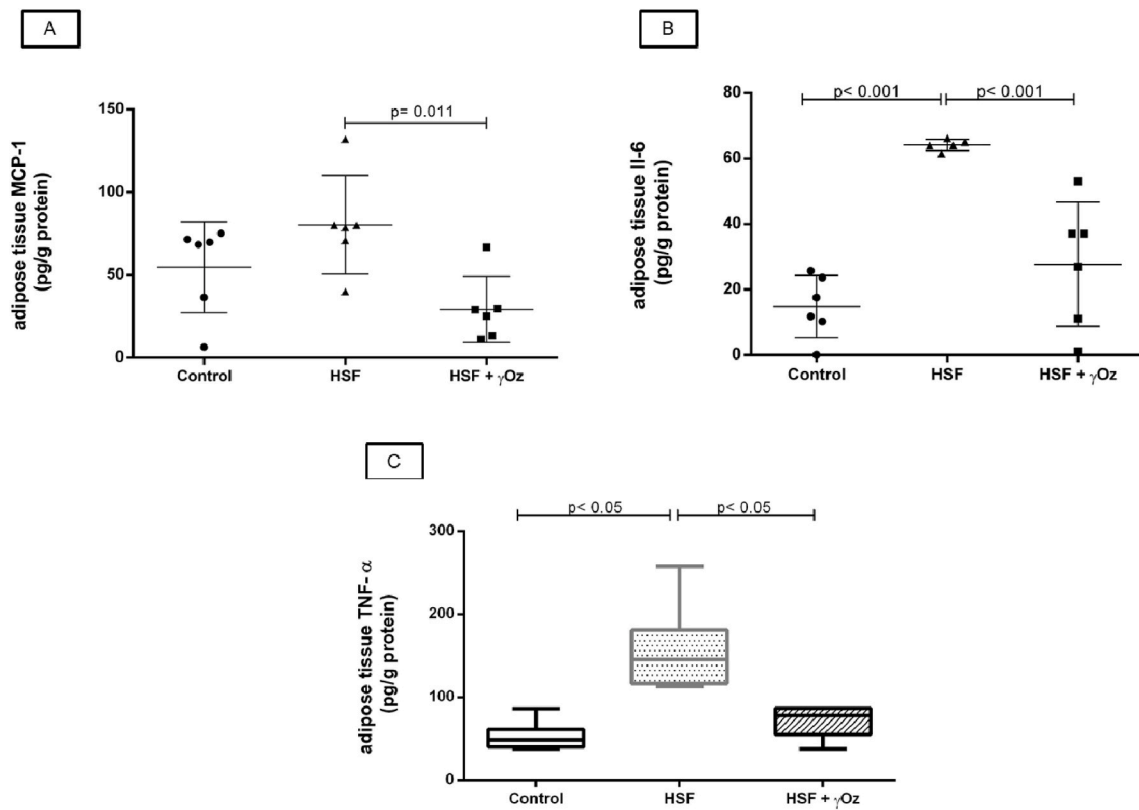


**Fig. 3.** Inflammatory parameters in epididymal adipose tissue. A- MCP-1 (pg/g protein); B- IL-6 (pg/g protein); C- TNF-  $\alpha$  (pg/g protein). Data expressed in mean  $\pm$  standard deviation or median with interquartile range. Comparison by One-way ANOVA with Tukey or Kruskal- Wallis post-hoc. HSF—high sugar- fat diet.  $\gamma$ Oz—Gamma-oryzanol.

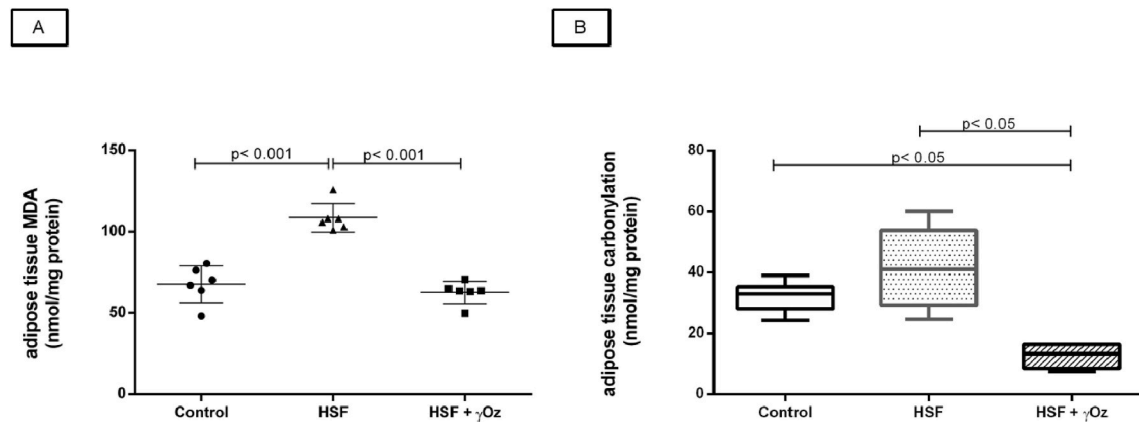


**Fig. 4.** Epididymal adipose tissue oxidative stress parameters. A- MDA: Malondialdehyde levels; B- carbonylation levels. Data are presented as means  $\pm$  standard deviation or median with interquartile range. Comparison by One-way ANOVA with Tukey or Kruskal- Wallis post-hoc. HSF—high sugar- fat diet.  $\gamma$ Oz—Gamma-oryzanol.

**2.10.2. Western blot**

Adipose tissue samples were homogenized in RIPA buffer with a protease and phosphatase cocktail inhibitor. After determination of protein concentration by the Bradford method (Bradford, 1976), samples were diluted in Laemmli buffer and loaded (25  $\mu$ g of protein) into a 12% SDS-polyacrylamide gel. Transfer to a nitrocellulose membrane was carried out using Trans-Blot Turbo-Transfer System (BioRad). Incubation with the primary antibodies was performed overnight at 4  $^{\circ}$ C in Tris-buffered saline solution containing Tween 20 (TBS-T) and 3% bovine serum albumin. Antibody dilutions were 1:1000 for PPAR- $\gamma$  (Santa Cruz Biotechnology E-8 sc- 7273) and 1:1000 for beta-actin (ABCAM ab8227). After incubation overnight at 4  $^{\circ}$ C in TBS-T

containing 1% nonfat dried milk with the Abcam secondary antibodies (dilution 1:1000 for anti-mouse and for anti-rabbit). Protein was revealed using the chemiluminescence method according to the manufacturer’s instructions (ECL SuperSignal $^{\circ}$  West Pico Chemiluminescent Substrate, Thermo Scientific). Band intensities were evaluated using ImageQuant TL 1D Version 8.1 (GE Healthcare Life Sciences).

**2.10.3. Statistical analysis**

Data are presented as means  $\pm$  standard deviation (SD) or median (interquartile range). Differences among the groups were determined by One-way analysis of variance. Parametric variables were subjected to the Tukey post-hoc test to compare all the groups. Non-parametric

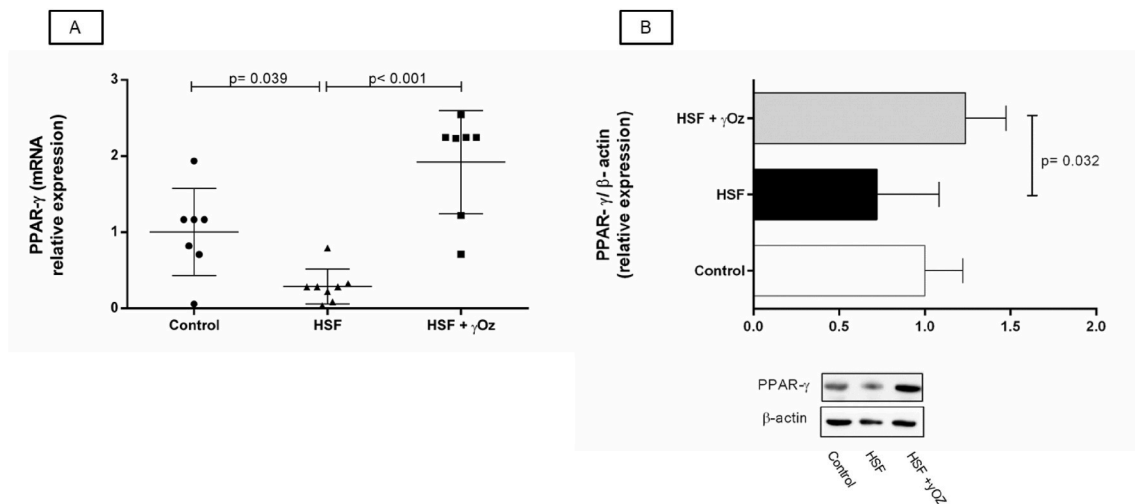


**Fig. 5.** Adipose tissue PPAR- $\gamma$  expression. A-gene expression by Real time PCR; B- protein expression by Western Blot. Data are presented as means  $\pm$  standard deviation. Comparison by One-way ANOVA with Tukey post-hoc. HSF—high sugar-fat diet.  $\gamma$ Oz—Gamma-oryzanol.

variables were compared by Kruskal-Wallis post-hoc test. Statistical analyses were performed using Sigma Stat for Windows Version 3.5. (Systat Software, Inc., San Jose, CA, USA). A  $p < 0.05$  was considered as statistically significant.

### 3. Results

**Table 1** presents the nutritional, hormonal and cardiometabolic parameters. Both groups that received the HSF diet presented lower chow fed and higher water intake compared to control group with no difference for caloric intake among the groups. The HSF group presented increased final body weight, adiposity index, fasting glucose, insulin, HOMA-IR, triglycerides, systolic blood pressure, leptin and adiponectin compared to control group. The treatment with  $\gamma$ Oz attenuated adiposity index, fasting glucose, HOMA-IR, triglycerides and leptin compared to the HSF group.

**Fig. 1** presents the histological analysis. The HSF group presented adipocyte hypertrophy, while the group treated with  $\gamma$ Oz showed the same adipocyte area and cell number/field as the control group.

**Fig. 2** presents the adipose tissue inflammatory markers. It is possible to verify that the HSF group presented increased MCP-1, IL-6 and TNF- $\alpha$  levels. However, the  $\gamma$ Oz demonstrated a positive anti-inflammatory effect, represented by reduced cytokines levels in the HSF +  $\gamma$ Oz group.

Adipose tissue malondialdehyde and protein carbonylation are presented in **Fig. 3**. The HSF group presented higher MDA levels compared to control group. In opposition, the HSF +  $\gamma$ Oz presented reduced MDA and protein carbonylation levels compared to HSF group.

Echocardiogram analysis showed that the treatment with  $\gamma$ Oz protected against cardiac remodeling, as showed by the left ventricular mass and relative wall thickness and also against systolic dysfunction, represented by the preserved ejection fraction. This positive effect occurred even in the systolic hypertension condition (**Fig. 4**).

Adipose tissue PPAR- $\gamma$  gene and protein expression are presented in **Fig. 5**. It is possible to note that  $\gamma$ Oz positively modulates both gene and protein expression in the HSF +  $\gamma$ Oz group.

### 4. Discussion

This study brings important findings regarding the positive effect of  $\gamma$ Oz to positively modulate the PPAR- $\gamma$  expression in adipose tissue, reducing the cytokines levels. This effect may act against the cytokine storm induced by obesity and COVID-19 infection.

PPAR- $\gamma$  is responsible by controlling several processes, such as adipogenesis, lipolysis, inflammation, glucose regulation and lipid

metabolism. Thus, any disruption in this receptor function can lead to adipose tissue dysfunction, usually associated with metabolic disorders, as insulin resistance (Corrales et al., 2018). Confirming the literature, the HSF group presented reduced PPAR- $\gamma$  expression and insulin resistance and high triglycerides and leptin levels. In opposition, the HSF +  $\gamma$ Oz group maintained the same PPAR- $\gamma$  expression as the control group and an attenuation of metabolic disorders compared with HSF. This is an important finding, especially in COVID-19 patients, since the presence of obesity-related comorbidities are associated with negative outcomes (Costa et al., 2020).

PPAR- $\gamma$  is also involved in adipose tissue inflammatory response, since the upregulation of this nuclear factor inhibits the TNF- $\alpha$  and IL-6 expression, suppresses macrophage infiltration into AT and induces polarization to an anti-inflammatory M2 (Thomas and Apovian, 2017). Confirming this finding, the HSF group presented higher levels of MCP-1, IL-6 and TNF- $\alpha$ , whereas the HSF +  $\gamma$ Oz group was protected against inflammation. Another explanation to the reduced inflammatory parameters levels is the reduction in malondialdehyde and protein carbonylation, both oxidative stress markers. Oxidative stress may affect extra-cellular matrix remodeling, mitochondrial respiration, cell proliferation and stimulate the nuclear factor kappa B (NF $\kappa$ B) to secrete cytokines. Moreover, oxidative stress affects repair mechanisms and the immune control system, which is one of the main events of the inflammatory response (Colitti et al., 2019).

The histological analysis demonstrated that the HSF +  $\gamma$ Oz group presented hyperplasia while the HSF, hypertrophy. This condition is beneficial to inflammation control, since in hyperplastic conditions are observed reduced cellular stress and synthesis of cytokines. PPAR- $\gamma$  is a crucial regulator of adipocyte differentiation and fat storage as triglycerides. Studies demonstrate that the PPAR- $\gamma$  is necessary for fat cell differentiation in all adipose depots and contributes to define the maximum threshold of expansion of the adipose tissue (Rosen et al., 1999; Semple et al., 2005). Moreover, in obesity condition, the PPAR- $\gamma$  expression decreases, which limits the adipose tissue expansion with consequent induction of cytokines production and fibrosis (Corrales et al., 2018). Studies show positive effects of PPAR- $\gamma$  activation in the treatment of cytokine storm induced by severe influenza, and this effect is associated to the anti-inflammatory and antioxidant modulation by this nuclear factor (Bassaganya-Riera et al., 2010; Liu et al., 2016).

In summary, this study showed that  $\gamma$ Oz attenuates metabolic syndrome, inflammation and oxidative stress in adipose tissue, which may be attributed to PPAR- $\gamma$  modulation. In addition, risk factors associated to COVID-19 severity as cardiac dysfunction and obesity progression were remarkable reduced in animals feeding  $\gamma$ Oz. Although future

studies to verify the  $\gamma$ Oz ability to ligate in PPAR- $\gamma$  are necessary, it is possible to conclude that  $\gamma$ Oz may be considered as therapeutic adjuvant to avoid/attenuate the systemic cytokine storm in COVID-19.

## Funding

São Paulo Research Foundation (FAPESP), grant #2015/10626-0 and #2018/15294-3.

## Data availability

The datasets generated during and/or analyzed during the current study are available from the corresponding author on reasonable request.

## Author contributions

**Conceptualization:** Francisqueti- Ferron FV; Minatel IO; Correa CR

**Data curation:** Francisqueti- Ferron FV; Ferron AJT; Minatel IO; Correa CR

**Formal analysis:** Francisqueti- Ferron FV; Minatel IO; Ferron AJT; Correa CR; Ferreira ALA

**Funding acquisition:** Correa CR

**Methodology:** Francisqueti- Ferron FV; Garcia JL; Lo ATC; Ferron AJT; Silva CCVA; Santos KC; Costa MR; Nakandakare-Maia ET; Gregolin CS; Silva JPC; Mattei L; Siqueira JS; Paula BH; Sarzi F; Moreto F

**Project administration:** Correa CR

**Supervision:** Minatel IO; Correa CR

**Writing - original draft:** Francisqueti- Ferron FV; Minatel IO; Correa CR.

## Declaration of competing interest

The authors declare no conflict of interest.

## References

- Abbas, A.M., Fathy, S.K., Fawzy, A.T., Salem, A.S., Shawky, M.S., 2020. The mutual effects of COVID-19 and obesity. *Obes Med* 19, 1–2.
- Almond, M.H., Edwards, M.R., Barclay, W.S., Johnston, S.L., 2013. Obesity and susceptibility to severe outcomes following respiratory viral infection. *Thorax* 68, 684–686.
- Ayres, J.S., 2020. A metabolic handbook for the COVID-19 pandemic. *Nat Metab* 2, 572–585.
- Bassaganya-Riera, J., Song, R., Roberts, P., Hontecillas, R., 2010. PPAR- $\gamma$  activation as an anti-inflammatory therapy for respiratory virus infections. *Viral Immunol.* 23, 343–352.
- Birsoy, K., Festuccia, W.T., Laplante, M., 2013. A comparative perspective on lipid storage in animals. *J. Cell Sci.* 126, 1541–1552.
- Bradford, M.M., 1976. A rapid and sensitive method for the quantitation of microgram quantities of protein utilizing the principle of protein-dye binding. *Anal. Biochem.* 72, 248–254.
- Chiappetta, S., Sharma, A.M., Bottino, V., Stier, C., 2020. COVID-19 and the role of chronic inflammation in patients with obesity. *Int. J. Obes.* 1–7.
- Ciavarella, C., Motta, L., Valente, S., Pasquinelli, G., 2020. Agonists of PPAR- $\gamma$  as candidates for cytokine storm modulation in COVID-19 disease. *Molecules* 25, 1–15.
- Colitti, M., Stefanon, B., Gabai, G., Gelain, M.E., Bonsembiante, F., 2019. Oxidative stress and nutraceuticals in the modulation of the immune function: current knowledge in animals of veterinary interest. *Antioxidants* 8, 1–19.
- Corrales, P., Vidal-Puig, A., Medina-Gómez, G., 2018. PPARs and metabolic disorders associated with challenged adipose tissue plasticity. *Int. J. Mol. Sci.* 19, 1–16.
- Costa, F.F., Rosário, W.R., Farias, A.C.R., Souza, R.G., Gondim, R.S.D., Barroso, W.A., 2020. Metabolic syndrome and COVID-19: an update on the associated comorbidities and proposed therapies. *Diabetes Metab Syndr Clin Res Rev* 14, 809–814.
- de Lucena, T.M.C., Santos, A.F. da S., de Lima, B.R., Borborema, M.E. de A., Silva, J. de A., 2020. Mechanism of inflammatory response in associated comorbidities in COVID-19. *Diabetes Metab Syndr Clin Res Rev* 14, 597–600.
- Finer, N., Garnett, S.P., Bruun, J.M., 2020. COVID-19 and obesity. *Clin Obes* 1–2.
- Francisqueti, Valentini, Fabiane, Nascimento, André Ferreira do, Corrêa, C.R., 2015. Obesidade, inflamação e complicações metabólicas. *Nutrire* 40, 81–89.
- Francisqueti, F.V., Minatel, I.O., Ferron, A.J.T., Bazan, S.G.Z., Silva, V. dos S., Garcia, J. L., et al., 2017a. Effect of gamma-oryzanol as therapeutic agent to prevent cardiorenal metabolic syndrome in animals submitted to high sugar-fat diet. *Nutrients* 9, 1–10.
- Francisqueti, F.V., Nascimento, A.F., Minatel, I.O., Dias, M.C., Luvizotto, R.D.A.M., Berchieri-Ronchi, C., et al., 2017b. Metabolic syndrome and inflammation in adipose tissue occur at different times in animals submitted to a high-sugar/fat diet. *J. Nutr. Sci.* 6, 1–8.
- Francisqueti, F.V., Junio, A., Ferron, T., Hasimoto, F.K., Henrique, P., Alves, R., et al., 2018. Gamma oryzanol treats obesity-induced kidney injuries by modulating the adiponectin receptor 2/PPAR- $\alpha$  axis. *Oxid Med Cell Longev* 2, 1–9.
- Fuentes, E., Guzmán-jofre, L., Moore-carrasco, R., Palomo, I., 2013. Role of PPARs in inflammatory processes associated with metabolic syndrome. *Mol. Med. Rep.* 8, 1611–1616.
- Goossens, G.H., Blaak, E.E., 2015. Adipose tissue dysfunction and impaired metabolic health in human obesity: a matter of oxygen? *Front. Endocrinol.* 6, 1–5.
- Instituto, I.B.G.E., 2011. Brasileiro de Geografia e Estatística, Coordenação de Trabalho e Rendimento. Pesquisa de Orçamentos Familiares: 2008-2009. Análise do Consumo Alimentar Pessoal no Brasil.
- Liu, Q., Zhou, Y., Yang, Z., 2016. The cytokine storm of severe influenza and development of immunomodulatory therapy. *Cell. Mol. Immunol.* 13, 3–10.
- Livak, K.J., Schmittgen, T.D., 2001. Analysis of relative gene expression data using real-time quantitative PCR and the 2<sup>- $\Delta\Delta$ CT</sup> method. *Methods* 25, 402–408.
- Manna, P., Jain, S.K., 2015. Obesity, oxidative stress, adipose tissue dysfunction, and the associated health risks: causes and therapeutic strategies. *Metab. Syndr. Relat. Disord.* 13, 423–444.
- Mesquita, C.S., Oliveira, R., Bento, F., Geraldo, D., Rodrigues, J.V., Marcos, J.C., 2014. Simplified 2,4-dinitrophenylhydrazine spectrophotometric assay for quantification of carbonyls in oxidized proteins. *Anal. Biochem.* 458, 69–71.
- Minatel, I.O., Francisqueti, F.V., Corrêa, C.R., Pace, G., Lima, P., 2016. Antioxidant activity of  $\gamma$ -Oryzanol: a complex network of interactions. *Int. J. Mol. Sci.* 17.
- Osman, O.S., Selway, J.L., Kępczyńska, M.A., Stocker, C.J., O'Dowd, J.F., Cawthorne, M. A., et al., 2013. A novel automated image analysis method for accurate adipocyte quantification. *Adipocyte* 2, 160–164.
- Rosen, E.D., Sarraf, P., Troy, A.E., Bradwin, G., Moore, K., Milstone, D.S., et al., 1999. PPAR $\gamma$  is required for the differentiation of adipose tissue in vivo and in vitro. *Mol. Cell.* 4, 611–617.
- Samarghandian, S., Farkhondeh, T., Samini, F., Borji, A., 2016. Protective effects of carvacrol against oxidative stress induced by chronic stress in rat's brain, liver, and kidney. *Biochem Res Int* 1–7.
- Santos, P.P. Dos, Rafacho, B.P.M., Gonçalves, A.D.F., Jaldin, R.G., Nascimento, T.B. Do, Silva, M.A.B., et al., 2014. Vitamin D Induces increased systolic arterial pressure via vascular reactivity and mechanical properties. *PLoS One* 9, 1–9.
- Semple, R.K., Meirhaeghe, A., Vidal-Puig, A.J., Schwabe, J.W.R., Wiggins, D., Gibbons, G.F., et al., 2005. A dominant negative human peroxisome proliferator-activated receptor (PPAR) $\alpha$  is a constitutive transcriptional corepressor and inhibits signaling through all PPAR isoforms. *Endocrinology* 146, 1871–1882.
- Son, M.J., Rico, C.W., Nam, S.H., Kang, M.Y., 2011. Effect of oryzanol and ferulic acid on the glucose metabolism of mice fed with a high-fat diet. *J. Food Sci.* 76, 4–7.
- Soy, M., Keser, G., Atangündüz, P., Tabak, F., Isik, A., Kayhan, S., 2020. Cytokine storm in COVID-19: pathogenesis and overview of anti-inflammatory agents used in treatment. *Clin. Rheumatol.* 1–10.
- Stefan, N., Birkenfeld, A.L., Schulze, M.B., Ludwig, D.S., 2020. Obesity and impaired metabolic health in patients with COVID-19. *Nat. Rev. Endocrinol.* 16, 341–342.
- Thomas, D., Apovian, C.M., 2017. Macrophage functions in lean and obese adipose tissue. *Metabolism* 72, 120–143.
- Wang, O., Liu, J., Cheng, Q., Guo, X., Wang, Y., Zhao, L., et al., 2015. Effects of ferulic acid and  $\gamma$ -oryzanol on metabolic syndrome in rats. *PLoS One* 10, 1–14.
- World Health Organization, 2017. WHO | Obesity and overweight. Fact Sheet N°311.
- Zabetakis, I., Lordan, R., Norton, C., 2020. COVID-19: the Inflammation Link and the Role of Nutrition in Potential Mitigation, vol. 2, pp. 1–28.